Analysis of the Inter-Stage Signal Leakage in Wide BW Low OSR and High DR CT MASH ΔΣM

Liu, Qilong ; Breems, Lucien J.; Bajoria, Shagun; Bolatkale, Muhammed; Zhang, Chenming; Radulov, Georgi

DOI
10.1109/ISCAS45731.2020.9180951

Publication date
2020

Document Version
Final published version

Published in
2020 IEEE International Symposium on Circuits and Systems (ISCAS)

Analysis of the Inter-stage Signal Leakage in Wide BW Low OSR and High DR CT MASH ΔΣM

Qilong Liu[1], Lucien J. Breems[1,2], Shagun Bajoria[2], Muhammed Bolatkale[2,3], Chenming Zhang[2], Georgi Radulov[1]
[1]Eindhoven University of Technology, Department of Electrical Engineering, The Netherlands, Email: Qilong.Liu@tue.nl
[2]NXP Semiconductors, Eindhoven, Eindhoven, The Netherlands
[3]Delft University of Technology, Delft, The Netherlands

***Abstract*—This paper analyzes the error mechanisms that limit the dynamic range (DR) of wide-bandwidth, low-OSR continuous-time (CT) multi-stage noise-shaping (MASH) ΔΣM and proposes a tool, the Signal Leakage Function (SLF), to optimize the architecture, and hence improving DR. The SLF provides new insights on finding the key parameters which influence the inter-stage signal leakage and thus the inter-stage gain (IG). These insights would lead not only to increasing the overall dynamic range in a very power-efficient way, but also decreasing the performance sensitivity to mismatches and other variations.**

I. Introduction

Owing to the progress in digital wireless communication, the demand for high-dynamic range (DR) wideband ADCs is increasing. A CT MASH ΔΣM can be a suitable architecture for these requirements. Thanks to the inter-stage gain (IG), the DR of all the sub-stages are optimally utilized. In common with single-stage implementation, CT MASH ΔΣMs also benefit from features such as resistive input and inherent anti-aliasing filtering. By cascading low-order ΔΣM sub-stages, the trade-offs between OSR, loop stability and design complexity can be relaxed [1]. This eventually makes CT MASH promising candidates for high DR, wide bandwidth applications with low OSR, which is very important for power efficiency.

However, some inherent disadvantages of the CT MASH architecture can limit its application. Besides the well-discussed noise leakage, as in [2][3][4], the signal leakage, which is often ignored, becomes a dominant problem in the wideband, low OSR context. To clarify this, Fig. 1 (a) shows an exemplary 2-stage MASH. The quantization noise is extracted by subtracting the input (y) of the quantizer from its output ($d1$). Due to the finite speed of the quantizer operating at several GHz, a certain delay (t_{QZ}) has to be tolerated between y and $d1$ to meet the metastability requirements. As the signal frequency increases, such a delay is translated as a phase shift of the signals, which causes uncancelled signal leakages, as shown in Fig. 1(b) and (c).

This signal leakage is detrimental for CT MASH to achieve high DR. If a large signal leakage shows up at the input of the second stage, IG must be reduced to avoid overloading. Compared to the leakage-free case, noise shaping becomes less aggressive, which counteracts the benefits of CT MASH.

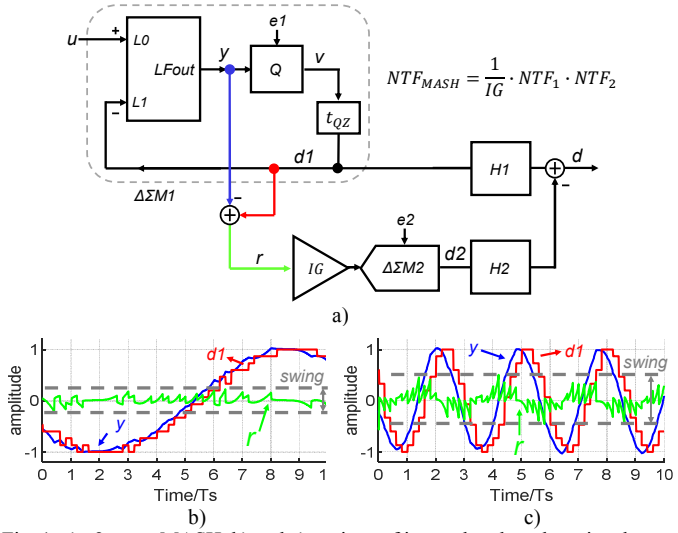

Fig. 1. a): 2-stage MASH. b) and c): swings of internal nodes when signal frequency is low and high, respectively

To alleviate this problem, RC and LC lattices have been proposed to balance the delay between the signal subtraction paths [5] [6]. Measurement results prove practical possibility to control the leakage. However, topics such as delay variation tolerance, parameter sensitivity and influence on the architecture choice are not theoretically analyzed in the literature. In this paper, the most important factors that determine the signal leakage are covered, namely delay mismatch and gain mismatch. The main challenge that our paper addresses is how to optimally design the inter-stage gain (IG). Our analysis and conclusions can be used further as a guidance for the performance optimization of CT MASH modulators.

This paper is organized as follows. Section II proposes a generic model for quantization noise extraction in CT MASH. Based on that a new metric called as Signal Leakage Function (SLF) is derived. Section III validates the efficacy of SLF. Section IV provides a design example using SLF as guidance to achieve high DR in a robust way. Section IV concludes the paper.

II. Derivation of Signal Leakage Function

A. Overview

Fig.2 shows a general model for quantization noise extraction in a CT MASH. Signal input, u, is sent to the loop

978-1-7281-3320-1/20/$31.00 ©2020 IEEE

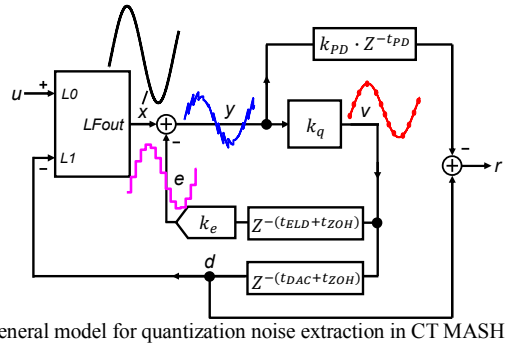

Fig. 2. General model for quantization noise extraction in CT MASH

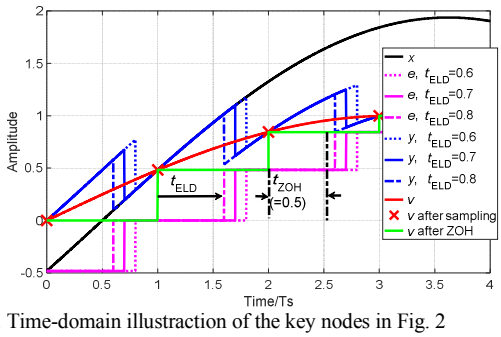

Fig. 3. Time-domain illustration of the key nodes in Fig. 2

via transfer function *L0* while the quantizer output (*d*), is fed back via transfer function *L1*. To compensate for excess-loop delay (ELD), a fast feedback path, *v* to *e*, is introducted around the quantizer with its own delay t_{ELD}. To meet the metastability requirement, a dedicated time, t_{DAC}, is added between quantizer's sampling moment and DAC's switching moment. In order to balance the quantizer delay between *y* and *d*, propagation delay is inserted intentionally with its delay as t_{PD}.

Assume both ELD compensation loop (*v* to *e*) and main feedback loop (*d,* through *L1* to *x*) are implemented with non-return-to-zero (NRZ) pulse shaped DACs. t_{ZOH} is added to desribe the half-clock period delay due to NRZ. Both $t_{ZOH}$and t_{ELD} are normalized to clock period *Ts*. All the aforementioned nodes (*d*, *e*, *r*, *u*, *v*, *x* and *y*) are analyzed in the CT domain with state variable *s*, which is also normalized to clock frequency. Furthermore, shorthand expression $z^{-1}=e^{-j\cdot s}$ is used as the continous-time representation of 1 *Ts* delay.

Fig. 3 shows the time-domain illustration of the key nodes in Fig.2. We find that for the ELD compensation loop (*v* through *e* to *y*), no matter how t_{ELD} varies between 0 and 1, the quantizer always sees exactly one-clock delayed *v* at the sampling moment, plus the output from the loopfilter (*x*). We can write:

$$v = k_q \cdot (x - k_e \cdot v \cdot z^{-1}) \tag{1}$$

where k_q, k_e represent the coefficients of the quantizer and ELD compensation loop, respectively.

However, as can be seen in Fig.3, the actual swing of *y* does vary as t_{ELD} shifts. To calculate the swing at *y*, the actual delay $z^{-t_{ELD}}$ should be used as a replacement of z^{-1} in (1):

$$y = x - e = x - k_e \cdot v \cdot z^{-(t_{ELD}+t_{ZOH})} \tag{2}$$

Likewise, for node *d*:

$$d = v \cdot z^{-(t_{DAC}+t_{ZOH})} \tag{3}$$

Now, we define Signal Leakage Function (SLF) to describe the residual signal seen at node *r*, which is:

$$SLF \coloneqq r/u = (d - y \cdot k_{PD} \cdot z^{-t_{PD}})/u \tag{4}$$

k_{PD} is the gain coefficient associated with the propagation delay path (*y* to *r*). Furthermore, noticed that ratio (v/u) is nothing but signal transfer function (STF):

$$STF \coloneqq v/u \tag{5}$$

Substitute (1)-(3) and (5) into (4). SLF is reduced to:

$$SLF = STF \cdot [z^{-t'_{DAC}} - k_{PD}/k_q \cdot z^{-t_{PD}} + k_e \cdot k_{PD} \cdot z^{-t_{PD}} \cdot (z^{-t'_{ELD}} - z^{-1})] \tag{6}$$

Furthermore, approximations below hold when the signal frequency of interest is much smaller than 1/*Ts*:

$$\begin{cases} z^{-t'_{ELD}} \approx 1 - t'_{ELD} \cdot s \\ z^{-t'_{DAC}} \approx 1 - t'_{DAC} \cdot s \\ z^{-t_{PD}} \approx 1 - t_{PD} \cdot s \end{cases} \tag{7}$$

Now SLF is approximated as:

$$\boxed{SLF \approx STF \cdot (\delta_r + T_r \cdot s)} \tag{8}$$

where

$$\boxed{\begin{aligned} \delta_r &= 1 - k_{PD}/k_q \\ T_r &= t_{PD} - t'_{DAC} - k_e \cdot k_q \cdot (t'_{ELD} - 1) \end{aligned}} \tag{9}$$

From (8), we find that SLF directly links three key metrics in a ΔΣM: STF, δ_r which corresponds to gain mismatch, and T_r, which is associated with delay mismatch. Since $STF \approx 1$ in the signal bandwidth, the following discussion mainly focuses on δ_r and T_r, with the aim of DR optimization for CT MASH.

Before preceding to the next section, the validity range of (6) and (8) should be mentioned. Firstly, in the derivation of (6), only the phase shift of ZOH is considered. The omission of its amplitude response gives less than 0.3dB error if fin<0.15 Fs. Secondly, in (1) it is assumed that node *x* contains only signal in the 1st Nyquist region, which is valid when anti-aliasing of *L1* is sufficient. Last but not least, in (6) and (8), the low-frequency approximation (7) should hold. The above three assumptions confine the validity range of SLF, which should be carefully checked as per use case.

III. Validation of Signal Leakage Function

To verify SLF, a simple 1st-order modulator (MOD1) with a numerical model is assumed, as shown in Fig. 4. Comparing with the model in Fig.2, more parameters are introduced to enhance modelling accuracy. The values of the parameters are listed in Tab. I. Note that t_{ELD}=1*Ts is chosen based on the discrete-time model, where the quantizer sees exactly one-clock cycle delayed *y* at its input, while t_{PD} =1*Ts is used to compensate such delay without any signal leakage.

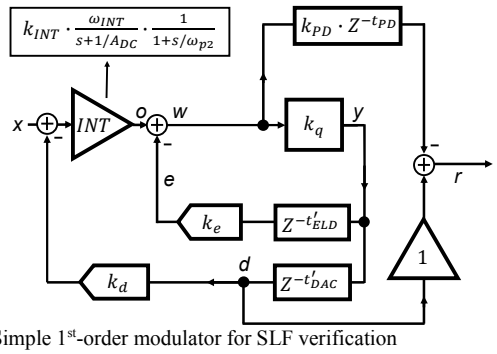

Fig. 4. Simple 1st-order modulator for SLF verification

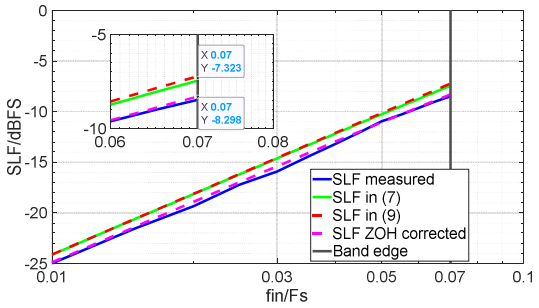

Fig.5 Simulated/calculated SLF's versus fin when $t_{PD} = 1$ Ts

Table. I Default values of the parameters in an ideal MOD1(t_{ZOH}=0.5 Ts)

Coeff.	Val.	Coeff.	Val.	Coeff.	Val.
k_d	1	t_{DAC}	1 Ts	A_{DC}	Inf.
k_e	1	t_{ELD}	1 Ts	t_{ZOH}	0.5 Ts
k_{PD}	1	t_{PD}	1 Ts	k_q	1
k_{INT}	1	w_{INT}	Fs/(2*π)	w_{p2}	Inf.

The signal leakage is measured at node r after passing through an 8th-order elliptic filter. This filter rejects out-of-band images to mimic inherent anti-aliasing of the next sub-stage ΔΣM. In order to avoid tonal behavior due to the low-order loop filter [1], an ideal 8-bit quantizer is simulated in order to correctly capture the signal amplitude. Finally, in order to expose signal leakage in the high-speed, high-bandwidth and power-efficient context, OSR is chosen to be as low as 7 without the loss of generality.

A. Verification of SLF

To simulate SLF, full-scale (0 ~ VDD, single-ended) sine wave is injected at MOD1's input. Note that since $k_e = k_q = 1$ as given in Tab. I, the gain mismatch factor δ_r would be zero. This indicates that only the delay mismatch factor T_r plays a role. Fig. 5 plots multiple simulated and analytically calculated SLF's from equation (8). The x-axis is the input frequency while y-axis is the signal leakage amplitude in dBFS. As it can be noticed, all the lines ramp up with a slope of 20dB/decade. This high-pass characteristic is correctly predicted by (8) when δ_r is set to be 0. Only 0.2dB difference is observed between the SLF's calculated via (6) and (8), which validates the low-frequency approximations in (7). Offset of about 1 dB exists between the simulated and the calculated examples. That is due to the omission of the amplitude response of ZOH in (6). After taking this factor into account, the corrected SLF (pink line in Fig.5) almost overlays with the simulation results. Since the offset is an order of magnitude smaller than the bulk part of SLF, we can continue using (8) as guidance for leakage optimization.

As clearly seen in Fig. 5, due to the high-pass characteristic of $T_r \cdot s$, the signal leakage reaches its maximum at the band edge. The large residual signal of -8.5 dBFS limits the IG and lowers the DR of the overall MASH. It strongly suggests the need of delay mismatch optimization.

B. Optimization of delay mismatch via SLF

In order to optimize the delay mismatch T_r, proper tuning mechanisms should be found. Among the parameters in T_r, t_{DAC} is often fixed by the metastability requirement. Following t_{DAC}, k_e is defined by the NTF characteristic of the sub-stage, which leaves t_{ELD} and t_{PD} as possible design freedoms.

Fig. 6 plots SLF's having t_{ELD} as 1*Ts and 0.5*Ts separately. The x-axis is the input frequency while the y-axis is the simulated/calculated SLF at the signal band edge, which is the worst case as explained III.A. It can be seen that all the SLF's are V-shaped, which agrees with the trend of $|T_r \cdot s|$ in (8). As t_{PD} increases, T_r crosses zero from its negative to positive. Local minima of SLF is reached at $t_{PD,opt}$ when $|T_r|$=0. However, simulation shows 0.1*Ts ~ 0.2*Ts offset at $t_{PD,opt}$ when comparing with the calculation via (6) or (8). That can be explained by the approximations used in deriving SLF, which has been covered in Section II. Since the offset is an order of magnitude smaller than the bulk part of $t_{PD,opt}$, we can still take (6) and (8) as good estimation.

It is instructive to discuss the two t_{ELD}'s in Fig. 6. Suppose we keep using t_{ELD}=1*Ts (blue line in Fig. 6), then $t_{PD,opt1}$ for CT MOD1 should be located at 1.8*Ts other than 1*Ts as in the discrete-time model. By optimizing t_{PD} via SLF, additional 10dB suppression can be achieved. Furthermore, if t_{ELD} is programmable without compromising loop stability, even more signal suppression can be achieved. The red line in Fig. 6 gives an example when t_{ELD}=0.5*Ts. At $t_{PD,opt2}$, SLF has 34dB more suppression compared with the default setup in Tab. I. Such an improvement indicates higher DR can be achieved with few modifications on the available design. Equivalently speaking, for the target dynamic range and the signal bandwidth, lower OSR can be chosen and thus higher power efficiency can be achieved. Such improvements can only be gained via the knowledge of SLF.

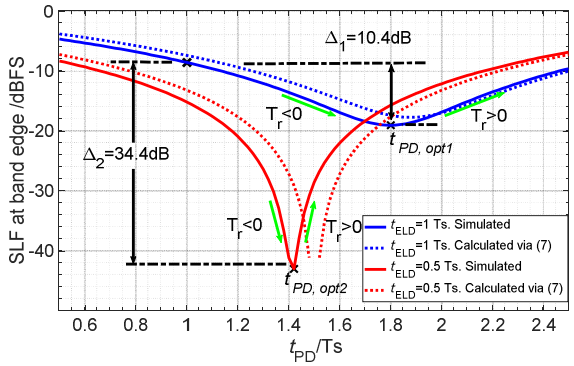

Fig. 6 SLF at band edge versus t_{PD}

C. *Importance of gain mismatch in SLF*

From (8) it can be seen, gain mismatch factor δ_r plays another important role in signal leakage reduction. To confirm that, simulations are done by assigning -10% ~ 10% variation to k_{PD}, while t_{PD}=1.42*Ts is chosen according to Fig 6. The simulated SLF's versus signal frequency is plotted in Fig. 7. Strong leakage can be observed even if k_{PD} only deviates by 10%, which completely ruins the improvement brought by T_r optimization. Such degradation can be intuitively understood by referring to Fig. 2: if either of the quantization noise extraction paths deviates by a small number delta, then the same amount of signal will bypass the subtraction node without cancellation. Thus 10%, 5% and 1% of Δk_{PD} will be translated as -20 dB, -26 dB and -40 dB leakages, respectively. Those values can be read from Fig.7. The accuracy of (8) is again verified. Sensitivity to k_q can be similarly explained, which is skipped for conciseness.

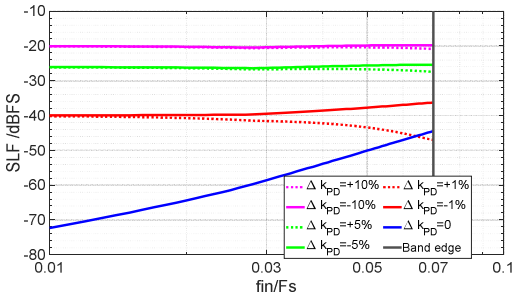

Fig. 7 SLF sensitivity to k_{PD} when t_{ELD}=0.5 Ts, t_{PD}=1.42 T

Lessons are learned from both T_r and δ_r analysis: in order to avoid overloading in CT MASH, measure should be taken to either guarantee the matching between the signal subtraction paths, or negotiate with IG for higher mismatch tolerance.

IV. Design Example

To prove the effectivness of SLF, multiple CT MASH are modeled and verified in MATLAB/Simulink. For comparison fairness, all the designs use 1-2 CT MASH with OSR=7. MOD1 serves as the first stage for its superior maximum stable amplitude. Simple 2nd-order feedback ΔΣM is used as the second stage without zero optimization [1]. 4-bit quantizators are implemented in both sub-stages. To mimic the R-C lattice in the real implementation [5], progation delay is replaced by an all-pass filter (APF) via approximation $e^{-t_{PD}\cdot s} \approx (1-\tau_{APF}\cdot s)/(1+\tau_{APF}\cdot s)$, where $\tau_{APF} = t_{PD}/2$. To align with the conclusions drawn above, simulations are carried out with $\{t_{ELD}, \tau_{APF}\}$ combinations as discussed in III.B. Depending on SLF, different IG's are employed and the resulted DRs' are compared. Fig. 8a plots the simulated spectrum of the three combinations. It can be found that, due to the unoptimized SLF in the default configuration (t_{ELD}=1*Ts, τ_{APF}=0.5*Ts), only 70dB DR can be achieved with the maximum IG=2.4V/V (black line). After applying τ_{APF}=0.9*Ts ($t_{TD,opt1}$=1.8*Ts as in Fig.6), IG can be increased to 6V/V and (6/2.4)=8 dB improvement can be observed (green line). Furthermore, if t_{ELD} can be designed to be 0.5*Ts, then DR can be further extended to 85 dB with IG=12V/V when τ_{APF}=0.71*Ts ($t_{TD,opt2}$=1.42*Ts as in Fig.6). Guided by SLF, we gain 15 dB[1] more DR by properly choosing t_{ELD} and optimizing τ_{APF}.

Fig. 8b shows 200 Monte Carlo runs with variations on MOD1's parameters as listed in Tab. II. The 3σ variation for gain and timing mismatch are set to 5% and 10% respectively. It gives the worst-case SLF would be -20dBFS at the signal bandedge, which is translated as IG=9V/V after taking quantization noise leakage into account. Simulated mean and 1σ value of DR is 83.2 dB and 1.7 dB respectively. No overloading is observed even in the worst case (78.7 dB). The simulation result confirms the effectiveness of SLF in CT MASH design.

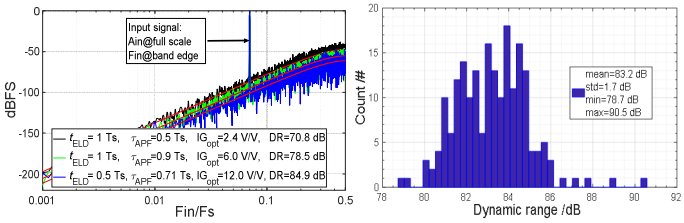

a) b)

Fig.8: a) Design exmaples with different $\{t_{ELD}, \tau_{APF}\}$ combinations;
b) DR distribution of 1-2 MASH with IG=9V/V after 200 MC runs;

Table. II Parameters used in the design example

coefficient	Centered value (m)	Standard variation (1σ)
k_d	1	0.01
k_e	0.67	0.008
k_{APF}	1.5	0.012
k_{INT}	1	0.01
k_q	1.5	0.012
A_{DC}	40 dB	1 dB
$TDAC/Ts$	200p s	Fixed
$TELD$	100p s	2.5p s
τ_{APF}	140p s	3.3p s
w_{INT}	3.3G rad/s	33M rad/s
w_{p2}	31.4G rad/s	500M rad/s

V. Conclusions

In this paper, a new metric, the Signal Leakage Function (SLF), is proposed to quantify the signal leakage in CT MASH ΔΣM and to optimize its dynamic range. As verified via analysis and numerical calculations, SLF is shown to be both intuitive and accurate to capture the key error mechanisms which limit the DR of the CT MASH ΔΣM. Using SLF as a design metric, a system-level example of a GHz-range ΔΣM is given with its robustness confirmed by Monte Carlo simulations. All the observations in the paper support SLF to be a convenient tool in the design of future CT MASH ΔΣMs.

[1] Ideal 34dB DR improvement shown in Fig. 6 cannot be reached. That is due to IG back-off to aviod quantization-noise-induced overloading. Since a 4-bit quantizer is used in the frist stage, IG would be limited below 16V/V if no dedicated action is taken to filter the out-of-band quantization noise. Aftering taking both signal leakage and quantization noise into account, the maximum IG is chosen to be 12V/V.

REFERENCES

[1] S. Pavan, R. Schreier, and G. C. Temes, *Understanding Delta-Sigma Data Converters*. John Wiley & Sons, 2017.

[2] L. J. Breems *et al*., "A cascaded continuous-time ΣΔM modulator with 67-dB dynamic range in 10-MHz bandwidth," *JSSC*, vol. 39, no. 12, pp. 2152–2160, 2004.

[3] Y.-S. Shu *et al*., "LMS-based noise leakage calibration of cascaded continuous-time ΔΣ modulators," *JSSC*, vol. 45, no. 2, pp. 368–379, 2010.

[4] C. Zhang *et al*., "A digital calibration technique for wide-band CT MASH ΣΔ ADCs with relaxed filter requirements," in *ISCAS*, 2016, pp. 1486 – 1489.

[5] Y. Dong *et al*., "A 72 dB-DR 465 MHz-BW continuous-time 1-2 MASH ADC in 28 nm CMOS," *JSSC*, vol. 51, no. 12, pp. 2917–2927, 2016.

[6] H. Shibata *et al.,* "A 9-GS/s 1.125-GHz BW oversampling continuous-time pipeline ADC achieving–164-dBFS/Hz NSD," *JSSC*, vol. 52, no. 12, pp. 3219–3234, 2017.